Heterochrony and Repurposing in the Evolution of Gymnosperm Seed Dispersal Units

Juca A. B. San Martin
Instituto de Botánica Darwinion: Instituto de Botanica Darwinion
Raúl Ernesto Pozner (rpozner@darwin.edu.ar)
Instituto de Botánica Darwinion: Instituto de Botanica Darwinion https://orcid.org/0000-0002-1467-1441
Verónica S. Di Stilio
University of Washington Seattle Campus: University of Washington

Research Article

Keywords: Bracts, Cellulosic Fibers, Fruit-like, Heterochrony, Histochemistry, Gnetales, Gymnosperm, Mucilage, Ontogeny, Seed dispersal.

Posted Date: October 19th, 2021

DOI: https://doi.org/10.21203/rs.3.rs-961637/v1

Abstract

Background: Plant dispersal units, or diaspores, allow the colonization of new environments, expanding geographic range and promoting gene flow. Two broad categories of diaspores found in seed plants are dry and fleshy, in connection to abiotic and biotic dispersal agents, respectively. Our understanding of the anatomical and developmental genetics of fleshy angiosperm fruits is fairly advanced, yet there is a knowledge gap for the analogous fleshy structures found in gymnosperm diaspores. Improved understanding of the structural basis of modified accessory organs that aid in seed dispersal will not only inform the evolution of this important trait in specific lineages but will also enable future work on the underlying genetics, contributing to hypotheses on the origin of angiosperm fruits.

To generate a structural framework for the development and evolution of gymnosperm fleshy diaspores, we studied the anatomy and histochemistry of *Ephedra* (Gnetales) seed cone bracts, the modified leaves surrounding the reproductive organs. We took an ontogenetic approach, comparing and contrasting the anatomy and histology of fleshy and papery-winged seed cone bracts in four closely related species in the South American clade, their pollen cone bracts, and leaves.

Results: Seed bract fleshiness in *Ephedra* derives from mucilage accumulated in chlorenchyma cells, also found in their reduced young leaves before they reach their mature, dry stage. Cellulosic fibers, an infrequent cell type in gymnosperms, were found in leaves and most bracts where they presumably function as a source of supplementary apoplastic water in fleshy seed cone bracts. Papery bract development more closely resembles that of leaves, which lack mucilage in this species, with further extension of hyaline margins into “wings”.

Conclusions: We propose an evolutionary developmental model whereby fleshy seed cone bracts result from a novel differentiation program repurposed from anatomical elements and compounds present in young leaves, whereas papery bracts derive from an extension of the mature leaf program. This model for the evolution of cone bract morphology in South American *Ephedra* hence involves changes in the timing of leaf differentiation, or heterochrony, that can further be tested in other gymnosperms with fleshy diaspores.

Background

Plants are sessile organisms with limited opportunities for gene flow, mainly via spores (the haploid stage) or seeds (the diploid stage). Seeds represent a major innovation in the history of land plants that enabled long-distance dispersal of a dormant embryo (the diploid sporophyte generation) wrapped in nutritive tissue, via abiotic or biotic agents. Extant seed plants consist of two major clades: gymnosperms, with naked ovules, and angiosperms, with ovules contained in ovaries that develop into fruits after pollination and fertilization. Angiosperm fruits have evolved highly diverse morphologies, with two broader categories consisting of dry vs. fleshy fruits. While gymnosperms do not have true fruits in the botanical sense, structures other than the angiosperm ovary can perform comparable functions in seed dispersal, similarly becoming fleshy or winged [1].

Strong selective pressures for the dispersal of progeny away from the maternal plant have led to multiple adaptations in seed dispersal units, or diaspores [2]. On the one hand, high elevation environments that typically exhibit high wind speeds, low vegetation cover and low animal density favor adaptations to wind dispersal such as winged, pappose, or light diaspores. On the other hand, lower elevation environments with higher vegetation cover and animal density favor dispersal by animals, typically in the form of fleshy diaspores [3]. Fleshy structures that aid in animal seed dispersal have evolved repeatedly and independently from different organs in gymnosperms, either within the ovule (such as the funicle or integuments), or accessory to it (such as bracts and pedicels) [4].

While there has been substantial progress in understanding the anatomical, developmental and genetic basis of angiosperm fleshy fruits [5], much less is known about analogous fleshy structures of multiple origin in gymnosperms [6, 7]. The idea that a basic genetic toolkit involving MADS box genes may be at play in all seed plant fleshy diaspores is appealing [8, 9]. However, addressing the potential co-option of genetic elements will require more in-depth knowledge of developmental morphology and anatomy in fleshy structures with distinct ontogenetic origin across gymnosperms. *Ephedra* (Gnetales) is an ideal system to investigate the evolution and development of fruit-like function in gymnosperms, since it includes species with fleshy and non-fleshy diaspores dispersed by animals or wind, respectively [10] (Fig. 1). A central argument for proposing to develop *Ephedra* into an evo-devo model lineage is indeed its contribution to the study of convergent fruit-like function in seed plants, by focusing on the fleshy character in non-angiosperm seed dispersal [11]. Within Gnetales, fleshy seed cone bracts are a distinctive ancestral feature found in *Ephedra* [13], where non-fleshy, papery winged or coriaceous seed cone bracts have arisen independently multiple times.

The *Ephedra* dispersal unit is the seed cone, found in female individuals of this dioecious gymnosperm, consisting of three pairs of decussate bracts and two ovules (except for a few species with three ovules and verticillate bracts) [12]. *Ephedra* seed cone bract anatomy and histology is relatively simple at the pollination stage (female gametophyte), typically consisting of a tanniniferous epidermis, a parenchymatous mesophyll (with or without fibers and tanniniferous cells), and two parallel vascular bundles surrounded by transfusion tissue [12]. This early pattern was presumed essentially equivalent between fleshy and non-fleshy bracts, except for the number of mesophyll layers and the width of the membranous margins [12]. However, upon closer scrutiny of descriptions across multiple species [12], we found that fleshy seed cone bracts can actually develop from different anatomies at the pollination stage: from parenchymatous mesophyll with or without tannins (e.g. *Ephedra equisetina*, *E. foeminea*, *E. minuta*, *E. saxatilis*) or from parenchymatous mesophyll with scattered (e.g. *E. fragilis*, *E. aphylla*, *E. altissima*) or subepidermal fibers (e.g., *E. tweediana*, *E. distachia*, *E. sarcocarpa*). This novel insight prompted us to conduct more detailed comparative work in order to clarify the developmental and structural basis of fleshy *Ephedra* bracts, and to contribute towards a better understanding of this important innovation. To that end, we included the investigation of putative homologous organs, pollen cone bracts (found in male individuals) and leaves, in order to gain a full evolutionary perspective.

Here, we investigate how seed accessory structures other than ovaries or ovules, become fleshy at the anatomical and histological level in the gymnosperm lineage *Ephedra*. To that end, we ask the following questions: (a) What is the developmental anatomy of fleshy seed cone bracts, and how does it differ from that of papery winged bracts, and non-fleshy pollen cone bracts?; (b) Are there new cell or tissue types associated with the development of fleshiness?; considering that cone bracts are modified leaves and hence homologous, (c) Do fleshy bracts share anatomical elements with leaves that suggest re-purposing? To address these questions, we studied seed cone bract development in four species of South American *Ephedra*, integrating morphology, anatomy and biochemistry in an ontogenetic framework. Fleshy seed cone bracts from three closely related species sister species *E. chilensis*, *E. triandra*, and *E. tweediana* were compared to their respective non-fleshy pollen cone bracts and vegetative leaves, and to papery winged seed cone bracts of *E. multiflora*. We end by summarizing our observations into a structural working model and speculate on the evolution of fleshy bracts from leaves in this intriguing gymnosperm lineage. Through the investigation of developmental patterns in fleshy and non-fleshy *Ephedra* diaspores, we uncovered more general processes such as anatomical repurposing and changes in developmental timing that help explain the emergence of this innovation.

Results

Given that bracts are modified leaves, and that the stages of anthesis and pollination (stage 1) are comparable for pollen and seed cone bracts, we present the results in the following order: seed cone bracts (stages 1 to 3), pollen cone bracts (stage 1), leaf anatomy and development, ending with histochemical analyses.

Developmental staging, comparative anatomy, and histology of seed cone bracts

Fleshy seed cone bracts differ in general morphology and anatomy from papery bracts since the early stage of pollination (stage 1). At developmental stage 1 (non-fleshy green) *Ephedra triandra* (Fig. 2) and *E. tweediana* (Fig. 3) seed cone bracts are wide triangular to wide ovate, with thin, hyaline margins and a thick, green central region running longitudinally (Figs. 2A and 3A). The adaxial (inner) epidermis had a similar structure to the abaxial (outer) epidermis, except that the latter had a thicker cuticle layer on the outer tangential walls (Figs. 2D and 3D-E). Sunken stomata are present on the abaxial epidermis only, while tanniniferous cells are found on both sides (Figs. 3D). Two longitudinal vascular bundles run along each bract, surrounded by transfusion tissue (Figs. 2D and 3D-E). The mesophyll consists of 4-5 layers of mucilage chlorenchyma abaxially (Figs. 2D and 3D-F) and one adaxial layer of cellulosic fibers, with vascular bundles running along the boundary (Figs. 2D and 3D-E). Mucilage chlorenchyma consists of cells with intense PAS and Alcian Blue staining in the central vacuole (Fig, 3F, Table 1 and Additional File 1). Bracts have 8 to 15-cell wide hyaline margins without mesophyll, consisting solely of an epidermis with adaxial cells that are mostly collapsed and reduced to their juxtaposed tangential walls (Fig. 3L).

From developmental stages 1 to 2, mucilage chlorenchyma cells became enlarged in both species (Figs. 2E-F, 3G-H). In *E. triandra*, several additional layers of cellulosic fibers developed under both sides of the epidermis (Fig. 2E-F, K). In *E. tweediana*, a second layer of subepidermal cellulosic fibers developed adaxially (Fig. 3G-I). Vascular bundles were found closer to the adaxial side of the bract, resulting in xylem and transfusion tissue being in direct contact with the cellulosic fibers (Figs. 2E-F, and 3G-I).

Seed cone bracts appeared to grow by expanding their green area at the expense of the hyaline margin, turning first red (Figs. 2B, E, F and 3B, G-I), and then fleshy (Figs. 2C, G-K, 3C, J-K). Throughout differentiation, mesophyll cells divided, expanded, and developed a large central vacuole, their mucilage content no longer identifiable with PAS (Figs. 2E-G, K, and 3J-K) nor Alcian blue (Table 1, Additional File 1). This process involved both cell division and expansion (Figs. 2G, K and 3J-K), since the number of mesophyll cell layers increased from 8-14 to up to 30. Subepidermal cellulosic fibers of *E. triandra* persisted as a continuous multilayer throughout bract differentiation (Fig. 2G-J). In *E. tweediana*, the subepidermal layer of cellulosic fibers did not follow bract expansion, separating instead into isolated bundles (Fig. 3J-K).

At developmental stage 1, *E. chilensis* seed cone bracts became fused at the base (Fig. 4A, C), their mesophyll consisting of 2-6 adaxial layers of cellulosic fibers and 4-6 abaxial layers of mucilage chlorenchyma (Fig. 4D-E). Anatomical changes from developmental stage 2 to 3, when bracts turn red and fleshy (Fig. 4B), also involved division and expansion of mucilage cells (Fig. 4F-G). Adaxial cellulosic fibers did not accompany bract expansion, resulting in their separation into several subepidermal bundles (Fig. 4F-G).

Ephedra multiflora seed cone bracts were already papery at stage 1 (Fig. 5A). They lack mucilage chlorenchyma and hence lack the gelatinous texture, instead developing extended papery hyaline margins, or “wings”. While the epidermis had the anatomical features described above for the fleshy species, little remained of the mesophyll in the middle region, which was reduced to two to three layers of subepidermal cellulosic fibers adaxially, and one to two adaxial tanniniferous layers, with both vascular bundles still discernible (Fig. 5C-F). The hyaline bract margins (55-60 cells wide) had no mesophyll, consisting solely of epidermis with collapsed cells on both sides, reduced to their juxtaposed tangential walls (Fig. 5C).

Comparative anatomy and histology of pollen cone bracts

Pollen cone bracts of fleshy species differ in general morphology and anatomy from those of the papery species since the early stage of pollination (stage 1). Pollen cone bracts of the fleshy species *Ephedra triandra* (Fig. 6A-D) and *E. tweediana* (Fig. 6E-F) had the same external morphology and internal anatomy. They are also similar to the seed cone bracts at stage 1, in terms of epidermis, abaxial stomata, vasculature, and margins (Fig. 6B-D and F). However, their mesophyll consists of 4-5 layers of compact parenchyma tissue adaxially and 4-5 layers of mucilage chlorenchyma abaxially (Fig. 6B-D and F). *Ephedra chilensis* pollen cone bracts (Fig. 6G) had similar external morphology to those of *E. triandra* and *E. tweediana* and similar epidermis and hyaline margin anatomy. The mesophyll differed in that it consisted of 2-6 adaxial layers of cellulosic fibers, and 1-2 abaxial layers of tanniniferous cells (Fig. 6H-I), and it did not include mucilage cells.

Pollen cone bracts of the papery species *E. multiflora* were wide-orbicular, dry, thin and membranous (Fig. 5A), with the same morphology and anatomy as seed cone bracts (data not shown).

Comparative anatomy and histology of leaves

Male and female individuals within a species share the same, highly reduced leaf morphology and anatomy, starting green and becoming dry and papery at maturity (Fig. 7A-D). Leaf development in *E. tweediana* can be summarized into six stages: (1) leaf primordium without hyaline margins and undifferentiated mesophyll; (2) leaf primordium with incipient hyaline margins (3-5 cells wide) and undifferentiated mesophyll; (3) young leaf with wider hyaline margins (7-15 cells wide), compact parenchyma and mucilage chlorenchyma; (4) compact parenchyma differentiated into cellulosic fibers; (5) mature leaf with hyaline margins, cellulosic fibers and tanniniferous cells; and (6) senescent leaf with loss of tanniniferous cells. Early stages of leaf development observed in *E. tweediana*, showed not only the development of the leaf primordium in terms of increased cell layers and size, but also the inception and progressive growth of the hyaline epidermal margin.

Young leaves (from the second node) of both sexes in *E. triandra*, *E. tweediana*, and *E. chilensis* developed hyaline, papery margins about 7-15 cells wide, consisting of overlapping adaxial and abaxial epidermis. The central longitudinal green area was relatively reduced, with the mesophyll consisting of 1-3 adaxial layers of compact parenchyma, 5-7 abaxial layers of mucilage chlorenchyma surrounding two vascular bundles, and transfusion tissue (Fig. 7E-L). In mature leaves, adaxial parenchyma differentiated into cellulosic fibers, and the mucilage cells found at young stages differentiated into tanniniferous cells (Fig. 7K-L). Cellulosic fibers and tanniniferous cells differentiated earlier in *E. chilensis* compared to *E. triandra* and *E. tweediana* (Fig. 7E-L), especially in leaves of male individuals. Young leaves of E. *multiflora* developed hyaline margins consisting of 7-12 cells wide and differentiated adaxial fibers and abaxial tanniniferous cells (Fig. 7M-N), reaching mature leaf anatomy relatively much earlier in development.

Histochemical analyses

Histochemical test results apply equally across comparable cell types in cone bracts and leaves (Table 1; Additional File 1). Cutin was detected in epidermal cell walls, non-crystalline cellulose and hemicellulose in primary walls, and pectin in the primary wall and middle lamellae, expected. Histochemical essays also revealed three unusual features: (1) Presence of mucilage inside chlorenchyma cells in young leaves and seed cone bracts (stage 1) of the fleshy species *E. chilensis*, *E. triandra* and *E. tweediana*, and in pollen cone bracts of *E. triandra* and *E. tweediana*; (2) Lack of lignin and presence of microcrystalline cellulose in the secondary walls of fibers; and (3) Lack of the typical storage molecules, starches, lipids, or proteins in both bracts and leaves.

Discussion

Here, we investigated the comparative anatomy of fleshy diaspores in South American *Ephedra*, an aspect of great relevance to their reproductive biology. We found that (1) Fleshy and papery seed cone bracts differ anatomically since early developmental stages, the former having mucilage chlorenchyma, (2) Mucilage underlies the gelatinous texture of fleshy seed cone bracts; (3) Cellulosic fibers are found in bracts, where they likely function as apoplastic water “pipes”, and (4) Young leaves and bracts share the same type of mucilage tissue in all fleshy species studied. We therefore propose that bract fleshiness is a novel differentiation program repurposed from mucilage tissue present in leaves, which develops similarly in all species. Additionally, we propose that the diversity of bract morphology and anatomy found in *Ephedra* likely evolved via heterochronic processes involving intra-individual changes in the timing of leaf developmental events.

Fleshy and papery seed cone bracts differ anatomically since pollination stage

Our ontogenetic observations and biochemical assays provide evidence that seed cone bracts from fleshy species develop previously undescribed, highly specialized mucilage chlorenchyma already discernible at the early stages of pollination, and not found in dry bracts at the same stage (Fig. 8A). This mucilage chlorenchyma can also be found in the bracts of pollen cones of the fleshy species, except for *E. chilensis*, where tanniniferous cells are found instead (Fig. 8B).

Mucilage accounts for the gelatinous texture of *Ephedra* fleshy seed cone bracts

Seed cone bracts of *E. chilensis*, *E. triandra* and *E. tweediana* have uniform, mucilage chlorenchyma mesophyll at the pollination stage (stage 1) that becomes distinctly red and fleshy at the seed dispersal stage (stage 3). Our histochemical assays identified mucilage as the substance responsible for the gelatinous texture of the mature red bracts of *E. chilensis*, *E. triandra* and *E. tweediana* seed cones. Mucilage comprises a family of highly branched, polymerized carbohydrates including L-arabinose, D-galactose, L-rhamnose, D-xylose, and galacturonic acid in various proportions that may also contain glycoproteins and other compounds such as tannins [14]. Whereas we found mucilage inside the cytoplasm of cells of a specialized type of parenchyma in *Ephedra*, mucilage is only found outside the cell, or in specialized cells known as idioblasts in angiosperms [15–17]. While our analysis was not able to detect the type and location of the pigment/s responsible for the red color at later developmental stages (stages 2 and 3), anthocyanins have been reported in fleshy red gymnosperm bracts and seeds [18], and rhodoxanthin is another good candidate found in *Ephedra monosperma* leaves [19].

Cellulosic fibers as apoplastic “water pipes”, an adaptation to arid environments

Another novel observation was the presence of cellulosic fibers in *Ephedra* cone bracts and leaves. Cellulosic fibers are similar to G-fibers in overall morphology, both are an infrequent cell type in gymnosperms only known otherwise from the wood of certain conifers [20], roots of cycads, and vegetative organs of Gnetales [21–25]. However, they have differences in structure and function: G-fibers or gelatinous fibers (also known as tension fibers) are long, fusiform, unbranched cells with lignified primary and secondary walls and a non-lignified innermost wall or gelatinous layer (Sg, or G-layer), composed mostly of lamellate cellulose [24]. Cellulosic fibers are also long and fusiform, but they are usually branched, with non-lignified primary and secondary walls and a tertiary wall of microcrystalline cellulose. In this study, we adopt “cellulosic fibers” to distinguish a particular type of fibers without lignin from the typical g-fibers, which usually differentiate in response to external forces, such as gravity or wind [24]. The specialized cell wall structure of G-fibers allows them to contract and produce counteracting tensile forces to reorient organs [26], as in Gnetales stems and roots [23]. Cellulosic fibers are only known for Gnetales within gymnosperms: as hypodermal fibers in *Welwitschia* leaves [21, 27], as cellulose fibers in *Gnetum* leaves [22], and also misidentified as g-fibers in the cortex of *Ephedra* stems [25]. In *Gnetum* leaves, cellulosic fibers perform a supplementary apoplastic water transport function to compensate for the low density of leaf veins [28], rather than the typical mechanical function. A water transport function is also compatible with a putative role in protecting axillary buds (leaves), and

reproductive strobili (pollen and seed cone bracts) against desiccation early in development, especially relevant in the semi-arid to arid environments inhabited by *Ephedra* in general [13], and the South American species in particular (Fig. 1). We therefore propose that this putative function of cellulosic fibers in leaves has been repurposed as a supplementary water supply system for the development of fleshy seed cone bracts that facilitate seed dispersal.

Shared leaf anatomy across species differs in the timing of maturation

Mature *Ephedra* leaves are typically reduced, scale-like, dry and membranous, and whither early; with photosynthetic function being transferred to the green stems [29]. These leaves consist of an epidermis collapsed to different degrees and lacking mesophyll, except in *E. altissima*, which develops linear leaves with little anatomical differentiation [29]. Our histological observations on leaves confirmed their reduced structure, while highlighting that they still contain distinct types of mesophyll cells at maturity: adaxial cellulosic fibers, abaxial tanniniferous cells, transfusion tissue and vascular tissue. This mature leaf anatomy is similar between male and female individuals of the same species, and between species with fleshy or papery seed cone bracts (Fig. 8C-D). Young (second node) leaves of fleshy species develop adaxial compact parenchyma and abaxial mucilage chlorenchyma prior to differentiating cellulosic fibers or tanniniferous cells, respectively. The transformation of chlorenchyma cells into tanniniferous cells is consistent with tannins being synthesized in chloroplast-derived organelles (tanossomes) [30, 31], and accumulating in the vacuole. Leaves of fleshy species appear to differ, however, in the timing of maturation (Fig. 9). Young leaves (second node) of the papery species *E. multiflora* already have mature anatomy, although we could not analyze leaves in the bud to verify whether mucilage chlorenchyma precedes tanniniferous cells (as in leaves of fleshy species), or whether they never form. Mucilage chlorenchyma in *E. multiflora* leaf primordia would account for a much earlier differentiation of leaf anatomy, while its absence would indicate a profound difference in foliar structure between fleshy and papery species. Despite being non-photosynthetic and highly reduced, mature *Ephedra* leaves are not completely dead structures, since tanniniferous cells are alive and cellulosic fibers can potentially continue to supply water via apoplastic transport. Considering all the evidence, mature leaves more likely perform a protective function towards axillary buds, against dehydration, heat, UV radiation [32] and herbivory [33].

Bract fleshiness is a novel differentiation program repurposed from leaves

Mucilage cells found in fleshy seed cone bracts are also found in young leaves, but while they turn into tanniniferous cells in leaves, they instead produce red pigment and expand into fleshy structures in seed cone bracts, presumably by increasing water intake. We propose that the terminal “leaf differentiation program” (mucilage cells becoming tanniniferous cells) fulfills a protective function that has been repurposed into a “fleshy bract differentiation program” (mucilage cells dividing, expanding, becoming fleshy and red) for a novel, seed dispersal role. Papery bracts of *E. multiflora* pollen and seed cones follow the differentiation program of leaves, as do pollen cone bracts of *E. chilensis* (Fig. 8).

Changes in the timing of leaf development drive seed cone bract diversification

Our results also revealed that reproductive bracts are anatomically more diverse than vegetative leaves in *Ephedra*, not due to new cell types, but to novel combinations enabling alternative differentiation pathways that depart from baseline leaf development. When comparing and contrasting bract and leaf anatomy (Fig. 8A-B vs. 8C-D), the structure of pollen cone bracts can be a) the same as seed cone bracts and leaves (*Ephedra multiflora*), b) different from seed cone bracts but similar to leaves (*E. chilensis*), or c) different from seed cone bracts and leaves (*E. tweediana* and *E. triandra*). Sexual dimorphism in cone bracts in the “fleshy species" is presumably related to their respective functions in pollen protection vs. animal seed dispersal via independent selective forces. At first sight, this reasoning appears to fail to explain why pollen and seed cone bracts of *E. multiflora* would be similar, until we consider the plant in its natural habitat: the selective pressures for dispersal by wind at high elevation desolate environments, where animals are scarce and wind speeds are high (Fig. 1G and Additional File 2).

From an ontogenetic perspective, bract diversity can be explained based on changes in the timing of leaf development. On the one hand, pollen and seed cone bract morphology resembles juvenile leaf shape with reduced hyaline margins in “fleshy species” (*E. chilensis, E. triandra* and *E. tweediana*) (Fig. 9A-D). The increase in cell layers between stages 2 and 3 of fleshy seed cone bracts leading to their maturity can be interpreted as a juvenile leaf developmental stage. Mesophyll of *E. chilensis* pollen cone bracts resembles mature leaf mesophyll (Fig. 9E and I), while that of *E. triandra* and *E. tweediana* matches young leaf anatomy (Fig. 9D and H). On the other hand, papery bracts of *E. multiflora* reflect senescent, or hypermature leaf features, both in their mesophyll anatomy and in the wide hyaline margins (Fig. 9F, J and K). Thus, bract structure in “fleshy species” may be interpreted as based upon juvenile

stages of leaf development, while that of “papery species” would result from the extension or acceleration of the mature leaf development program.

Heterochrony represents changes in the timing of developmental events leading to phenotypic variation between the ancestor and its descendants [34, 35]. While different types of heterochrony have been described: interspecific vs. intraspecific [36], growth vs. sequence [37], transcriptional vs. metabolic vs. cellular [38], all of them are framed in an evolutionary context (between ancestor and descendants), or among individuals of the same species. In our study, the proposed changes in the timing of developmental events would be modifying homologous structures on the same individual, since leaves and bracts are considered serial (iterative) homologous structures [39], yet the adoption of heterochrony for serially homologous structures has not been fully developed [40, 41]. In the meantime, ancestral character reconstruction at the genus level would further test the potential role of heterochrony in cone bract evolution in *Ephedra*.

Evolutionary considerations

Overall, bract anatomy was more nuanced than expected: remarkably similar between sister species *Ephedra tweediana* and *E. triandra* (for both pollen and seed cone bracts), yet markedly different from *E. chilensis* pollen cone bracts (sister species of *E. tweediana* + *E. triandra*) [13]. “Fleshy” seed cone bracts are considered the ancestral state for the South American clade, while dry papery bracts have presumably evolved independently multiple times in *Ephedra* [13], yet only once in the South American clade, in the branch leading to *E. multiflora* and *E. boelckei* [12, 13]. Here, we contribute anatomical and histological evidence for *Ephedra* cone bracts that suggests that the ancestral fleshy character state may represent a novel type of bract differentiation built upon young leaf anatomy, while the derived dry, papery bract state is based on an existing differentiation pattern found in mature vegetative leaves. Additionally, we propose that cellulosic fibers observed here in *Ephedra* leaves and bracts, and also found in *Gnetum* [22] and *Welwitschia* [21, 27], may constitute a previously overlooked valuable synapomorphy for the order Gnetales.

Conclusions

Our study revealed that fleshy and papery bracts differ anatomically from early stages of development and that they both share features with leaf anatomy. Mucilage, found in leaves and bracts at early developmental stages, provides the gelatinous texture in fleshy seed cone bracts. This mucilage appears to have been repurposed from a role in drought and freezing tolerance in leaves, to one in seed dispersal in cone bracts. Cellulosic fibers, also found in bracts and leaves, likely channel apoplastic water that hydrates the mucilage. Based on our observations, it seems likely that the two types of bract morphology in South American *Ephedra* arouse from heterochronic changes in leaf development: fleshy bracts from modifications to a young leaf program, and papery bracts from an acceleration/extension of the adult leaf program.

Materials And Methods

Plant materials

Reproductive branches were collected from male and female individuals of four dioecious species of *Ephedra* (Additional File 2) in natural populations in Northwest Argentina (La Rioja and Catamarca provinces) and fixed immediately in FAA (Formaldehyde : Alcohol : Acetic acid) [42]. Vouchers were deposited in the herbarium at Instituto de Botánica Darwinion (SI, Buenos Aires, Additional File 3), where samples were brought for processing and study. To test whether cone bract anatomy matches that of leaves, we compared young (green) and mature (brown) leaves from male and female individuals to pollen and seed cone bracts, respectively. To consistently compare similar developmental stages, we sampled the second pair of leaves from the shoot apex for the young stage, and brown leaves from unbranched basal nodes (5th or 6th node from the shoot apex) for the mature stage. Young and mature leaves of *E. tweediana*, *E. chilensis*, and *E. triandra* were fixed in FAA. Leaves of *E. multiflora*, and additional leaves for the remaining three species were sampled from herbarium vouchers, rehydrated and fixed following [43]. To further investigate the full scope of leaf development, we studied earlier developmental stages in *Ephedra tweediana* leaf primordia.

Anatomy and histology

Bract anatomy and histology was conducted in pollen cones (staminate, or male) and seed cones (ovulate, or female) of four species of *Ephedra* in an ontogenetic series. We identified three developmental stages in seed cone bracts: (1) non-fleshy green, (2) non-fleshy reddish (turning from green to red), and (3) fleshy red. Stage 1 was the longest, comprising most developmental processes, from young

ovule to advanced embryo. We chose bracts at the pollination stage (when ovules are green, with turgent micropylar tubes that secrete pollination drops) as a reference point for comparison among species within stage 1. In stage 2 the embryo is almost at its final size, and stage 3 corresponds to mature seeds before dispersal. Pollen cone bracts were studied at anthesis (the pollen-shedding stage, with bracts comparable to stage 1 seed cones). In order to compare the two bract types found in South America, papery winged seed cones of *Ephedra multiflora* were also analyzed at stages 1 and 3. Bracts and leaves at different developmental stages were dissected, dehydrated, and embedded in Technovit 7100 historesin (Kulzer GmbH, Wehrheim, Germany).Transverse sections 2-5 µm thick were obtained using a Jung 2055 microtome (Leica, Wetzlar, Germany) following [44].

Histochemistry

Tissue sections were stained with Toluidine blue and Periodic Acid Schiff reaction (PAS) for general structure analysis. PAS reaction was also used for the identification of total non-soluble polysaccharides, polarized light microscopy to identify microcrystalline cellulose, Lugol's iodine test for starch, Coomasie blue for proteins, Sudan black for lipids, Ruthenium red for pectins [42], and Alcian blue for mucilage [45]. We performed the same set of histochemical tests on bracts and leaves.

Microscopy and Photography

Digital images were taken with a Nikon FXA microscope and NIS-elements software, with enhanced contrast and white balance tools. Figures were assembled in Inkscape 1.0.

Declarations

Ethics approval and consent to participate

Not applicable.

Consent for publication

Javier Torréns and Adriana Aranda-Rickert consent to the publication of their photos in Fig. 1.

Availability of data and materials

All data generated or analyzed during this study are included in this published article, and its supplementary information files.

Competing interests

The authors declare that they have no competing interests

Funding

This study was funded by a National Geographic Society Research Grant (NGS-55332R-19) to VSD and RP; by a grant from the Ministerio de Ciencia, Tecnología e Innovación Productiva (ANPCyT, Argentina) PICT 2019-1816 to RP (co-PI), VDS (Raíces Program Investigator), and JSM (Collaborator Team); and a Fulbright USA-Argentina Scholar Award to VSD.

Authors' contributions

VSD designed the study, procured funding, collected samples in the field, took photographs of overall morphology and cowrote and edited the manuscript; RP directed the anatomical and histochemistry studies, prepared figures, cowrote and edited the manuscript, JSM conducted the histology, anatomy and histochemistry, prepared figures and formatted the manuscript.

Authors' information (optional)

Not applicable

Acknowledgements

We thank María Magdalena Brizuela for assistance with species localization and voucher collection, the Acosta family for hosting VSD and facilitating plant tissue collection in and around their property (El Rodeo, Catamarca, Argentina), Adriana Aranda-Rickert for photos

of *E. triandra*, and Agustín Sanguinetti (Universidad de Buenos Aires) for help with sample collection of *E. tweediana*.

References

1. Leslie AB, Beaulieu JM, Mathews S. Variation in seed size is structured by dispersal syndrome and cone morphology in conifers and other nonflowering seed plants. New Phytol. 2017;216:429–37. doi:10.1111/nph.14456.
2. Seale M, Nakayama N. From passive to informed: mechanical mechanisms of seed dispersal. New Phytologist. 2020;225:653–8. doi:10.1111/nph.16110.
3. Traveset A, Rodríguez-Pérez J. Seed Dispersal. In: Jørgensen SE, Fath BD, editors. Encyclopedia of Ecology. Oxford: Academic Press; 2008. p. 3188–94.
4. Nigris S, D'Apice G, Moschin S, Ciarle R, Baldan B. Fleshy Structures Associated with Ovule Protection and Seed Dispersal in Gymnosperms: A Systematic and Evolutionary Overview. CRC Crit Rev Plant Sci. 2021: 1–18. doi:10.1080/07352689.2021.1938397.
5. Pabón-Mora N, Litt A. Comparative anatomical and developmental analysis of dry and fleshy fruits of Solanaceae. Am J Bot. 2011; 98:1415–36.
6. Zumajo-Cardona C, Ambrose BA. Deciphering the evolution of the ovule genetic network through expression analyses in *Gnetum gnemon*. Ann Bot. 2021;:1–41. doi:10.1093/aob/mcab059.
7. Zumajo-Cardona C, Pabón-Mora N, Ambrose BA. The evolution of euAPETALA2 genes in vascular plants: from plesiomorphic roles in sporangia to acquired functions in ovules and fruits. Mol Biol Evol. 2021;38:2319–36. doi:10.1093/molbev/msab027.
8. Lovisetto A, Baldan B, Pavanello A, Casadoro G. Characterization of an AGAMOUS gene expressed throughout development of the fleshy fruit-like structure produced by *Ginkgo biloba* around its seeds. BMC Evol Biol. 2015;15:1–13. doi:10.1186/s12862-015-0418-x.
9. Lovisetto A, Guzzo F, Tadiello A, Toffali K, Favretto A, Casadoro G. Molecular analyses of MADS-box genes trace back to gymnosperms the invention of fleshy fruits. Mol Biol Evol. 2012;29:409–19.
10. Hollander JL, Vander Wall SB, Baguley JG. Evolution of seed dispersal in North American *Ephedra*. Evol Ecol. 2010;24:333–45.
11. Di Stilio VS, Ickert-Bond SM. Ephedra as a gymnosperm evo-devo model lineage. Evol Dev. 2021;23:256–66.
12. Rydin C, Khodabandeh A, Endress PK. The female reproductive unit of *Ephedra* (Gnetales): Comparative morphology and evolutionary perspectives. Bot J Linn Soc. 2010;163:387–430.
13. Ickert-Bond SM, Wojciechowski MF. Phylogenetic relationships in *Ephedra* (Gnetales): Evidence from nuclear and chloroplast DNA sequence data. Syst Bot. 2004;29:834–49.
14. Monrroy M, García E, Ríos K, García JR. Extraction and Physicochemical Characterization of mucilage from *Opuntia cochenillifera* (L.) Miller. J Chem. 2017;2017. doi:10.1155/2017/4301901.
15. Mastroberti AA, De Araujo Mariath JE. Development of mucilage cells of *Araucaria angustifolia* (Araucariaceae). Protoplasma. 2008;232:233–45. doi:10.1007/s00709-007-0274-7.
16. Mastroberti AA, De Araujo Mariath JE. Compartmented cells in the mesophyll of *Araucaria angustifolia* (Araucariaceae). Aust J Bot. 2003;51:267–74.
17. Mastroberti AA, Mariath JEDA. Immunocytochemistry of the mucilage cells of *Araucaria angustifolia* (Bertol.) Kuntze (Araucariaceae). Rev Bras Bot. 2008;31:1–13.
18. Rudall PJ. Colourful cones: how did flower colour first evolve? J Exp Bot. 2020;71:759–67. doi:10.1093/jxb/erz479.
19. Sofronova VE, Chepalov VA, Dymova O V., Golovko TK. The role of pigment system of an evergreen dwarf shrub *Ephedra monosperma* in adaptation to the climate of Central Yakutia. Russ J Plant Physiol. 2014;61:246–54.
20. Jourez B. Le bois de tension 1. Définition et distribution dans l'arbre. Biotechnol Agron Soc Environ. 1997;1:100–12.
21. Rodin RJ. Leaf anatomy of *Welwitschia*. II. A study of mature leaves. Am J Bot. 1958;45:96.
22. Tomlinson PB, Fisher JB. Development of nonlignified fibers in leaves of *Gnetum gnemon* (Gnetales). Am J Bot. 2005;92:383–9.
23. Tomlinson PB, Magellan TM, Griffith MP. Root contraction in *Cycas* and *Zamia* (Cycadales) determined by gelatinous fibers. Am J Bot. 2014;101:1275–85. doi:10.3732/ajb.1400170.
24. Magellan TM, Griffith MP, Tomlinson PB. Distribution of gelatinous fibers in seedling roots of living cycads. Am J Bot. 2015;102:1250–9. doi:10.3732/ajb.1500235.

25. Montes MM, Ewers FW, Bobich EG. Gelatinous fibres are not produced in response to induced stresses in *Ephedra*. IAWA J. 2015;36:121–37. doi:10.1163/22941932-00000090.
26. Mellerowicz EJ, Gorshkova TA. Tensional stress generation in gelatinous fibres: A review and possible mechanism based on cell-wall structure and composition. J Exp Bot. 2012;63:551–65. doi:10.1093/jxb/err339.
27. Rodin RJ. Anatomy of the reproductive bracts in *Welwitschia*. Am J Bot. 1963;50:641–8.
28. Zwieniecki MA, Boyce CK. The role of cellulose fibers in *Gnetum gnemon* leaf hydraulics. Int J Plant Sci. 2014;175:1054–61.
29. Dörken VM. Leaf-morphology and leaf-anatomy in *Ephedra altissima* DESF. (Ephedraceae, Gnetales) and their evolutionary relevance. Feddes Repert. 2014;123:243–55. doi:10.1002/fedr.201200020.
30. Brillouet JM, Romieu C, Schoefs B, Solymosi K, Cheynier V, Fulcrand H, et al. The tannosome is an organelle forming condensed tannins in the chlorophyllous organs of Tracheophyta. Ann Bot. 2013;112:1003–14.
31. Brillouet JM, Romieu C, Lartaud M, Jublanc E, Torregrosa L, Cazevieille C. Formation of vacuolar tannin deposits in the chlorophyllous organs of Tracheophyta: from shuttles to accretions. Protoplasma. 2014;251:1387–93. doi:10.1007/s00709-014-0640-1.
32. Suseela V. Potential roles of plant biochemistry in mediating ecosystem responses to warming and drought. In: Ecosystem consequences of soil warming. Elsevier; 2019. p. 103–24. doi:10.1016/B978-0-12-813493-1.00005-3.
33. Barbehenn R V, Constabel CP. Tannins in plant-herbivore interactions. Phytochemistry. 2011;72:1551–65.
34. Gould SJ. Ontogeny and phylogeny. Cambridge: Harvard University Press; 1977.
35. Alberch P, Gould SJ, Oster GF, Wake DB. Size and shape in ontogeny and phylogeny. Paleobiology. 1979; 5:296–317. doi:10.1017/S0094837300006588.
36. Reilly SM, Wiley EO, Meinhardt DJ. An integrative approach to heterochrony: The distinction between interspecific and intraspecific phenomena. Biol J Linn Soc. 1997; 60:119–43. doi:10.1006/bijl.1996.0092.
37. Smith KK. Heterochrony revisited: The evolution of developmental sequences. Biol J Linn Soc. 2001; 73:169–86.
38. Buendía-Monreal M, Gillmor CS. The times they are a-changin': heterochrony in plant development and evolution. Front Plant Sci. 2018; 9 September:1–8.
39. Baum DA. Plant parts: processes, structures, or functions? Gard Bull Singapore. 2019; 71 suppl.2:245–56.
40. Li P, Johnston MO. Heterochrony in plant evolutionary studies through the twentieth century. Botanical Review. 2000; 66:57–88.
41. Pryer KM, Hearn DJ. Evolution of leaf form in marsileaceous ferns: Evidence for heterochrony. Evolution (N Y). 2009; 63:498–513.
42. Ruzin SE. Plant microtechnique and microscopy. New York: Oxford University Press; 1999.
43. Venning FD. Manual of advanced plant microtechnique. Dubuque, Iowa.: Wm. C. Brown Company Publishers; 1953.
44. O'Brien TP, McCully ME. The study of plant structure: principles and selectd methods. Melbourne: Termacarphi Pty; 1981.
45. Steedman HF. Alcian blue 8GS: a new stain for mucin. Q J Microsc Sci. 1950; 91:477–9.
46. Erdtman G. Sporoderm morphology and morphogenesis. A collocation of data and suppositions. Grana. 1966;6:317–23.
47. Johansen DA. Plant microtechnique. New York: McGraw-Hill Book Co. Inc.; 1940.
48. Southworth D. Cytochemical reactivity of pollen walls. J Histochem Cytochem. 1973;21:73–80.
49. Jensen W. Botanical histochemistry: principles and practice. San Franscisco: W. H. Freeman and Company; 1962.
50. Zavala-Gallo L. Ephedraceae. In: Zuloaga FO, Belgrano MJ, editors. Flora Vascular de la republica Argentina. Vol2. 1st edition. San Isidro: Instituto de Botánica Darwinion; 2016. p. 391–401.

Tables

Table 1 – Summary of histochemical and microscopy tests on pollen and seed cone bracts.

Histochemical Test	Pollen Cone Bract				Seed Cone Bract				
	Epidermis	Fibers		Parenchyma	Epidermis (stage 1-3)	Fibers (Stage 1-3)		Parenchyma	
		Primary wall	Secondary wall			Primary wall	Secondary wall	(Stage 1-2)	(Stage 3)
Toluidine blue O	Green	Blue	Not stain	Blue	Green	Blue	Not stain	Blue	Blue
PAS	---	+++	---	+ + +	---	+++	---	+ + +	---
Alcian blue	---	---	---	+ + +	---	---	---	+ + +	---
Ruthenium Red	---	+ + +	---	---	---	+ + +	---	---	---
IKI (Lugol)	---	---	---	---	---	---	---	---	---
Polarized Light	---	+ + +	+ + +	---	---	+ + +	+ + +	---	---
Coomassie Blue R-2503	---	++-	---	+++ (Peripheral to vacuole)	---	++-	---	+++ (Peripheral to vacuole)	---
Sudan Black B	---	---	---	---	---	---	---	---	---

Cytochemical test specificity: Toluidine blue O - Polyanionic acid groups: blue, phenolic compounds: green, pectins: purple [46]; PAS - Insoluble polysaccharides [44]; Alcian blue - Mucilage [42, 45]; Ruthenium Red - Pectins and IKI (Lugol) - Starch [47]; Polarized Light - Birefringent crystalline fibers [48]; Sudan Black B - Lipids (including phospholipids) [49]. (+++) strong, (++-) positive, (+--) weak, (—) none observed.

Figures

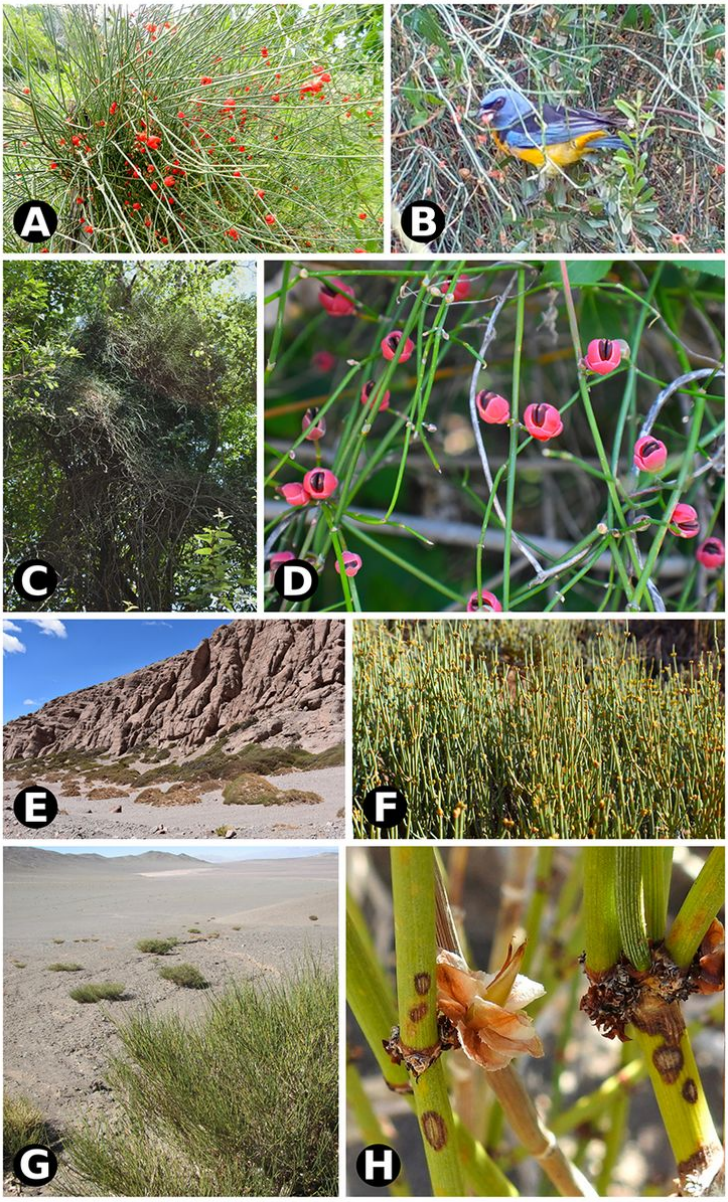

Figure 1

Natural environment, habit and dispersal biology of Ephedra species studied. (A-B) E. triandra with seed cones. (B) Bird disperser Rauenia bonariensis, “naranjero” feeding on fleshy cones (Anillaco, la Rioja); photos in (A-B) by Adriana Aranda-Rickert. (C) E. tweediana climbing on a tree; (D) Detail of fleshy cones (El Rodeo, Catamarca). (E) E. chilensis in high elevation semi-arid environment; (F) Plant detail (Laguna Brava, La Rioja). (G) Sparse populations of E. multiflora in high elevation semi-dessert environment; photo by Javier Torréns; (F) Detail of plant habit (Laguna Brava, La Rioja); photo by Adriana Aranda-Rickert.

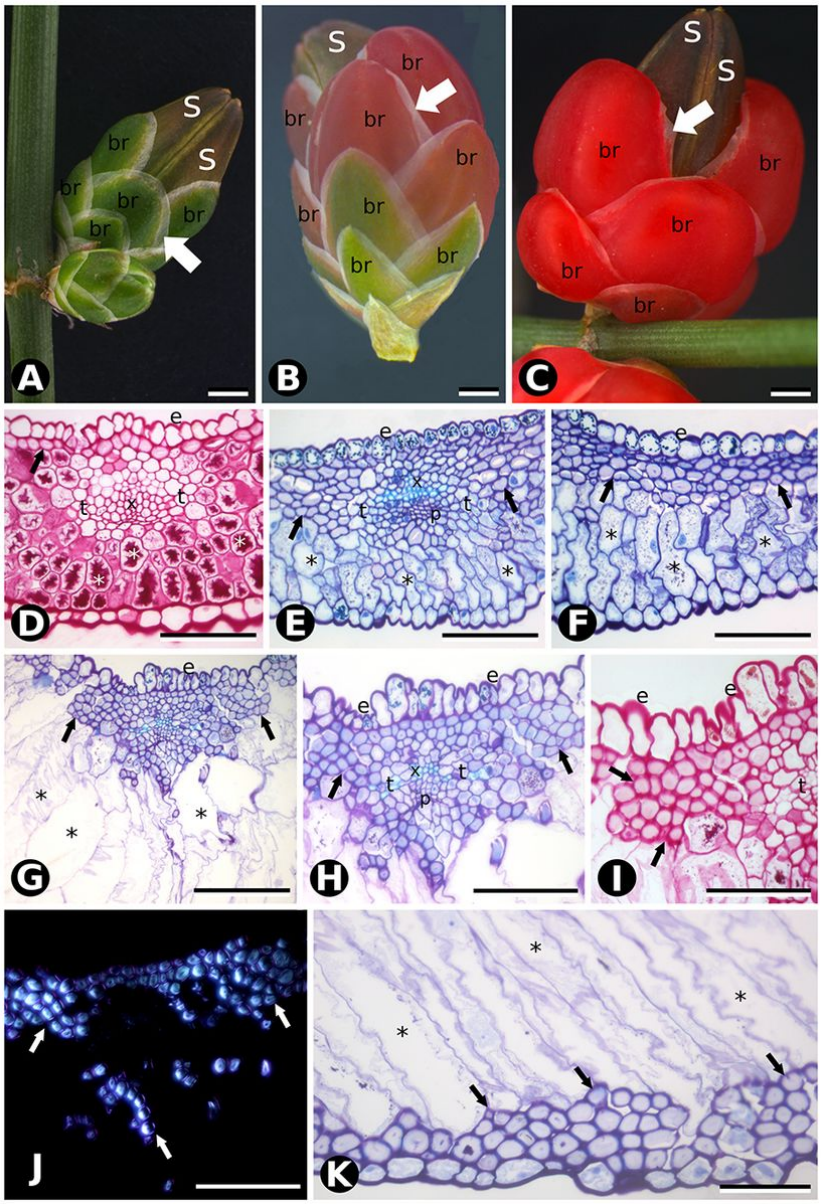

Figure 2

Comparative morphology and bract anatomy of Ephedra triandra seed cones at three key developmental stages: (A) Green (Stage 1) (B) Red (Stage 2) and (C) Fleshy (Stage 3). The white arrow shows a papyraceous lateral region that decreases as bracts (br) mature. (s) seed. (D) Cross section of a green bract stained with PAS showing a continuous single layer of cellulosic fibers beneath the epidermis (black arrow), and a mesophyll of cells with large amounts of insoluble carbohydrates (*). Adaxial epidermis (e), xylem (x) and transfusion tissue (t) (E-F) Cross sections of red bracts stained with PAS and Toluidine blue O, showing the proliferation of cellulosic fibers (black arrows) beneath the adaxial epidermis (e). Mesophyll cells (*) no longer contain insoluble carbohydrates. (G) Cross section of red and fleshy bracts showing an adaxial epidermis (e) with columnar cells and cellulosic fibers organized in several sub-epidermal layers (arrows). Mesophyll cells (*) look enlarged, with thin primary walls and enlarged vacuoles. (H) Detail of the vascular bundle in (G), adaxial epidermis (e), xylem (x) and transfusion tissue (t). (I) Detail of cellulosic fibers (arrows) showing intense PAS staining on their primary walls (black arrows) and lighter staining on their secondary walls. adaxial epidermis (e) and transfusion tissue (t). (J) Polarized light microscopy showing the intense birefringence of cellulosic fibers in cross-section (arrows). (K) Detail of the abaxial face showing the distribution of cellulosic fibers (arrows) in subepidermal layers. Mesophyll cells (*) are enlarged, with thin, sinuous walls and enlarged vacuoles in their cytoplasm. Scale bars: 1 mm (A-C); 100 µm (D); 50 µm (E-F, I, J and K); 100 µm (G-H).

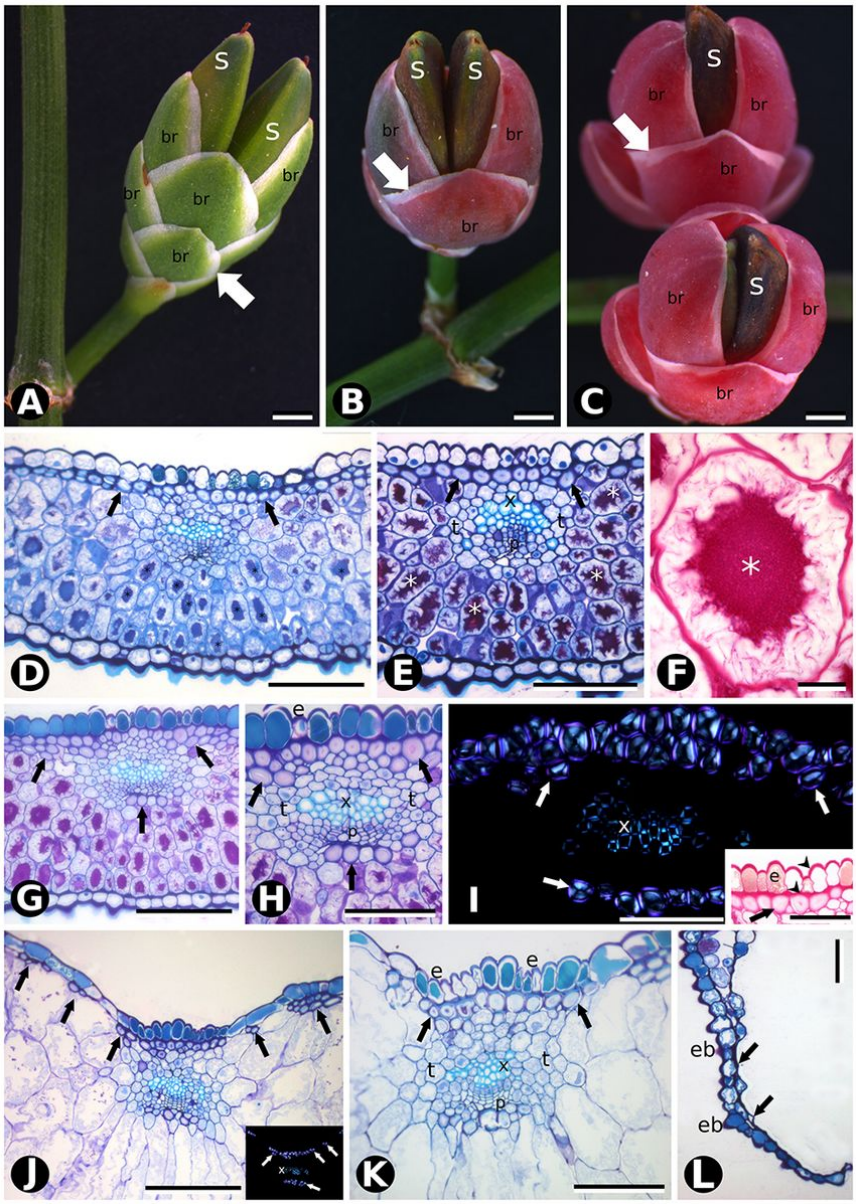

Figure 3

Comparative morphology and bract anatomy of Ephedra tweediana seed cones at three key developmental stages: (A) Green (Stage 1); (B) Red (Stage 2), and (C) Fleshy (Stage 3). White arrows show the papyraceous lateral region of the bracts (br); two seeds (s) are present per cone. (D) Cross section of a green bract stained with Toluidine blue O and PAS showing a homogeneous mesophyll consisting of cells with large amounts of insoluble carbohydrates (*) and cellulosic fibers (black arrows) distributed in a single adaxial sub-epidermal layer. (E) detail of vascular bundle in (D), with mesophyll cells with large amounts of insoluble carbohydrates (*), phloem (p), xylem (x) and transfusion tissue (t). (F) Detail of mesophyll cell stained with PAS showing its vacuole filled with insoluble carbohydrates (*). (G) Overview of a red bract in cross section showing an increase in the number of cellulosic fiber layers (black arrows). (H) Detail of the vascular bundle shown in (G), with adaxial epidermal cells (e) filled with phenolic compounds (tannins), and cellulosic fibers organized into one or two subepidermal layers (black arrows). (I) Polarized light microscopy showing the intense birefringence of cellulosic fibers in cross-section (white arrows). Inset, detail of cellulosic fibers showing intense PAS staining on primary walls (arrowheads) and weak staining on secondary walls (black arrow). Adaxial epidermis (e) with thickening of the external and internal periclinal walls (arrowheads). (J-L) Cross section of fleshy bracts (stage 3). (J) cellulosic fibers (black arrows) are organized in separate bundles of one or two layers beneath the adaxial epidermis. Mesophyll cells are large with thin, sinuous walls and devoid of cytoplasmic content. Inset: polarized light microscopy showing the intense birefringence of cellulosic fibers (white arrows) and xylem (x). (K) Detail of the vascular bundle area beneath the adaxial epidermis (e) with cellulosic fibers (black arrows) above, phloem (p), xylem (x) and transfusion tissue (t). (L) Detail of papery lateral region of the bract, consisting solely of epidermis, with

adaxial cells collapsed and reduced to the periclinal, juxtaposed walls (black arrows) and abaxial epidermis (eb) with tanniniferous cells. Scale bars: 1 mm (A-C); 100 µm (D-E, G, J-L); 50 µm (I); 20 µm (F).

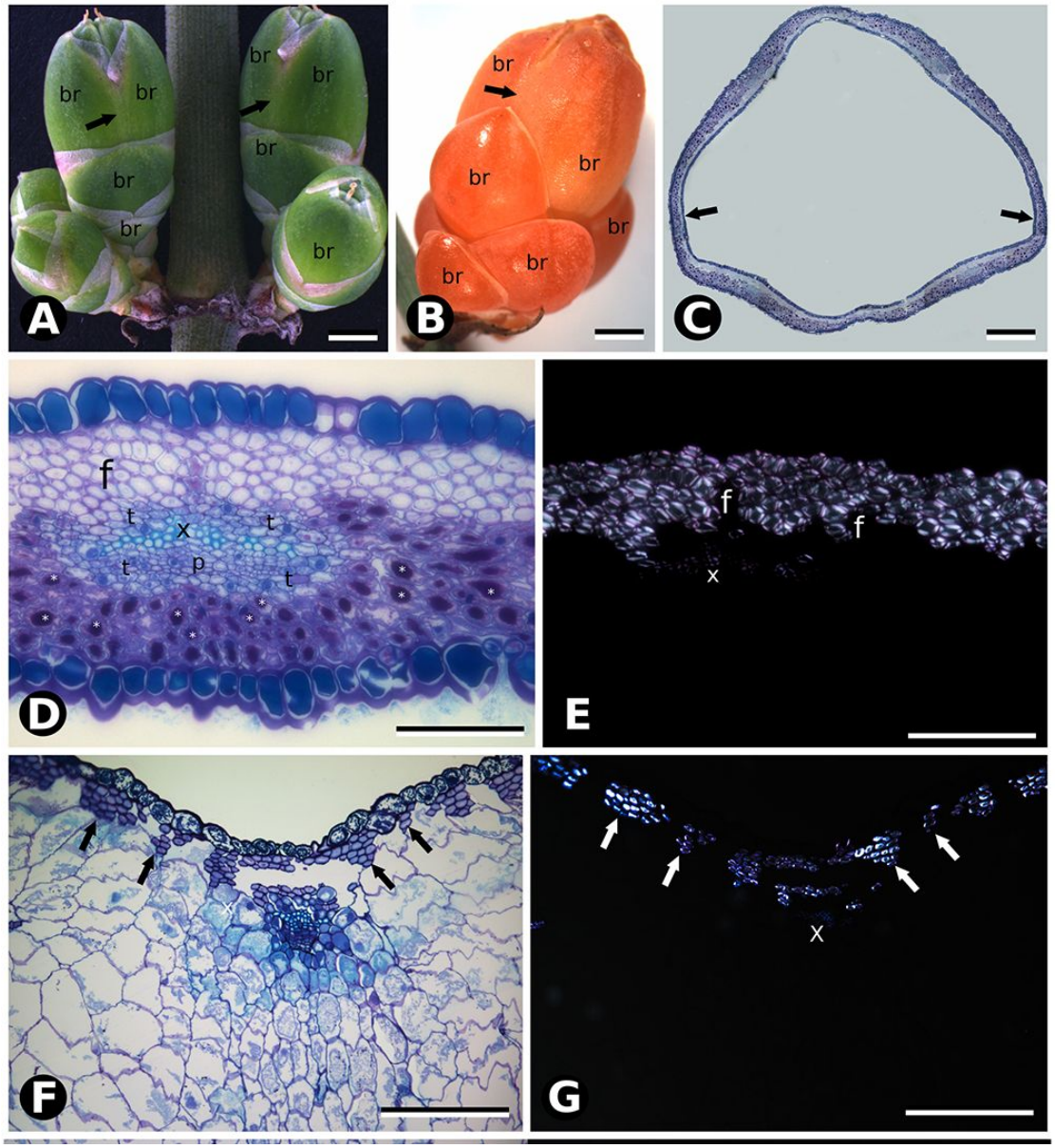

Figure 4

Comparative morphology and bract anatomy of E. chilensis seed cones. (A) Seed cone in stage 1, with green bracts (br). Black arrows indicate the fused region of the distal bracts. (B) Seed cone at stage 3, with fleshy red bracts (br). Black arrows indicate the fused region of the distal bracts. Note the highly developed distal bracts that completely enclose the seeds, which are not visible as in the other species studied. (C) Overview of anatomical section in the region of seed cone bract fusion (black arrows). (D) Cross section of seed cone bract at stage 1 stained with Toluidine Blue O and PAS showing large tannin content in cells of the adaxial epidermis. Cellulose fibers (f) are grouped into layers on the adaxial side. A vascular bundle is surrounded by transfusion tissue (t), phloem (p) and xylem (x). Mucilaginous parenchyma is evident abaxially, and the abaxial epidermis is composed of cells with tannins and stomata. (E) Polarized light microscopy of section in (D) showing the birefringence of cellulosic fibers (f) and xylem (x). (F) Cross section of the seed cone bract at stage 3 stained with Toluidine Blue and PAS showing increased of cell size and loss of carbohydrates from the cytoplasm of mucilaginous parenchyma cells. Fiber layers (arrows) are reduced in number and grouped in bundles beneath the adaxial epidermis. (G) Polarized light microscopy of the section in (F) showing the birefringence of cellulosic fibers (white arrows) and xylem (x). Scale bars: 1 mm (A-B); 200 µm (C); 100 µm (D-G).

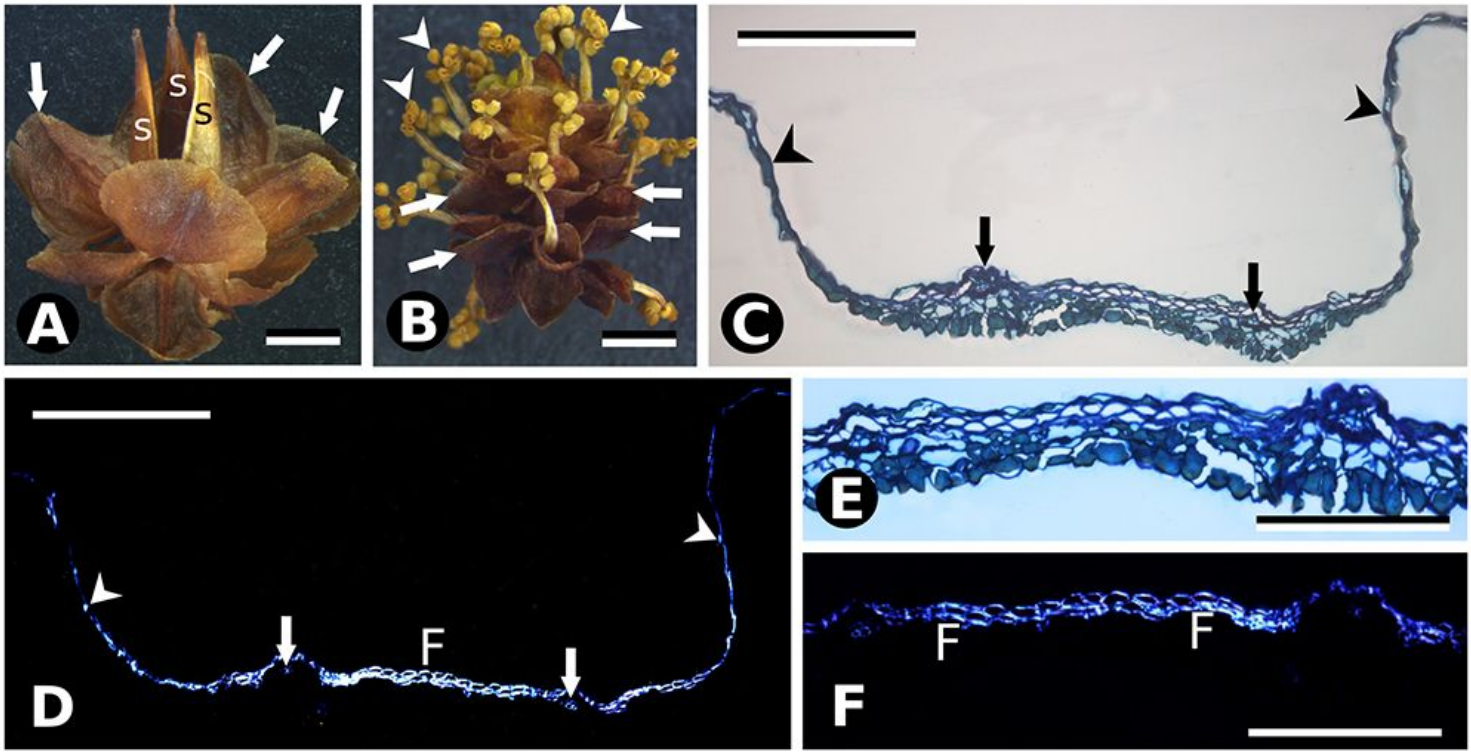

Figure 5

Morphology and anatomy of seed and pollen cones of E. multiflora in stage 3 of development. (A) Seed cone with three seeds (s) in the terminal region and papyraceous bracts (arrow). (B) Pollen cone after pollination with open microsporangia (arrowheads) and papyraceous bracts (arrows). (C) Cross section of the papyraceous seed cone bract at low magnification showing general appearance, stained with PAS and Toluidine Blue O. Arrows indicate the two vascular bundle and arrowheads indicate de lateral papyraceous area. (D) Polarized light microscopy of section in (C) showing the birefringent crystalline organization of cellulosic fibers (arrows show the two vascular bundles). (E and F) Detail of the central mesophyll region of figures (C) and (D), respectively, (f) cellulosic fibers. Scale bars: 1 mm (A-B); 100 µm (C-D); 50 µm (E-F).

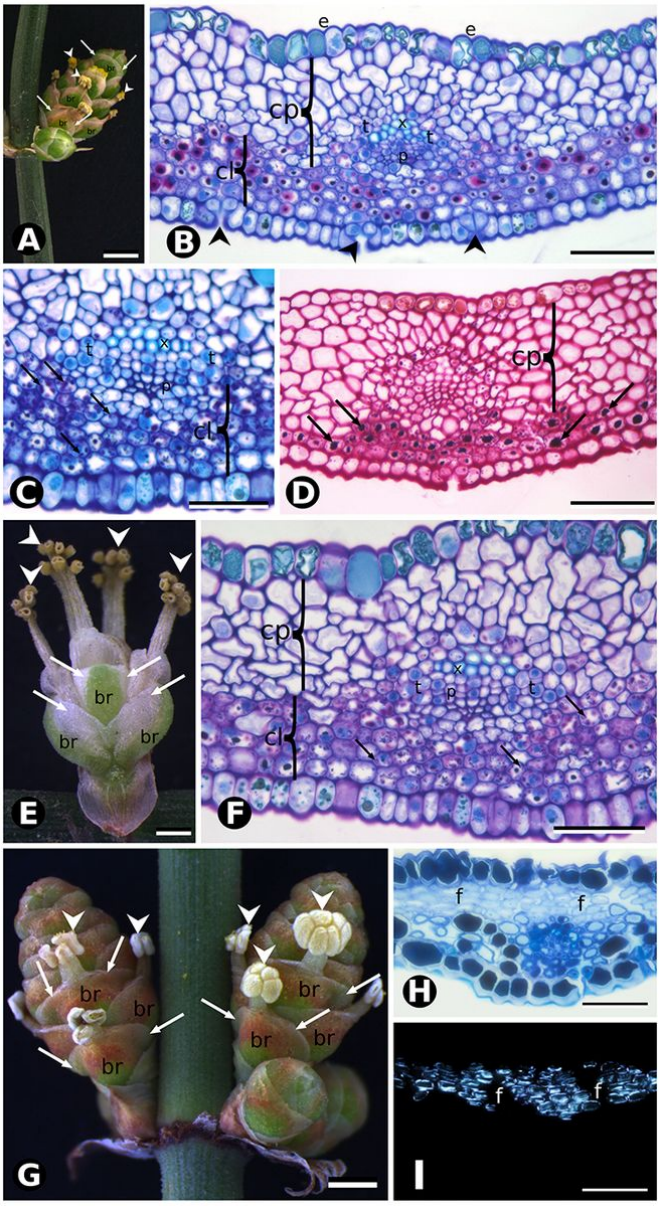

Figure 6

Comparative morphology and bract anatomy of the pollen cone of Ephedra triandra (A-D), E. tweediana (E-F) and E. chilensis (G-I). (A) Overall appearance of pollen cone of E. triandra after pollination, green bracts (br) with hyaline margins (arrows) enclose one microsporangiophore each (arrowheads), with multiple microsporangia (pollen sacs) at their tips. (B) Cross section through a pollen cone bract of E. triandra stained with Toluidine Blue O and PAS. The adaxial epidermis (e) consists of tanniniferous cells, with large phenolic content (tannin). The heterogeneous mesophyll consists of an adaxial, compact parenchyma (cp) without intercellular spaces and an abaxial chlorenchyma (cl) of cells containing large amounts of insoluble carbohydrates (mucilage) inside their vacuole, as evidenced by strong PAS staining (magenta to purple). A vascular bundle, with poorly developed phloem (p), xylem (x) and transfusion tissue (t) is found at the interface between the two parenchyma types. Stomata (arrowheads) are present in the abaxial epidermis. (C) Detail of the vascular bundle in cross section, stained only with Toluidine blue O. Chlorenchyma cells (cl) contain multiple chloroplasts each (arrows). (D) The same bract stained with PAS alone shows large amounts of insoluble carbohydrates (arrows) within chlorenchyma cells. (E) Pollen cone of E. tweediana after pollination. Green bracts (br) with white hyaline margins (arrows) enclose one microsporangiophore each (arrowheads), with multiple microsporangia (pollen sacs) at their tips. (F) Cross section of pollen cone bract stained with only Toluidine Blue O showing the same anatomical pattern as in E. triandra. (G) Pollen cone at anthesis of E. chilensis. Arrowheads indicate microsporangia at anthesis (left cone) and pre-anthesis (right cone), arrows show hyaline margins on bracts (br). (H) Cross section of a pollen cone bract at anthesis stained with Toluidine Blue O and PAS. The mesophyll consists of cellulosic fibers (f) and tanniniferous cells, insoluble carbohydrates (mucilage) are not observed within parenchyma cells in this species. (I) Polarized

microscopy of bract section in (H) showing birefringence of cellulosic fibers (f). Scale bars: 1 mm (A, E, G); 50 µm (C, H, I); 100 µm (B, D, F).

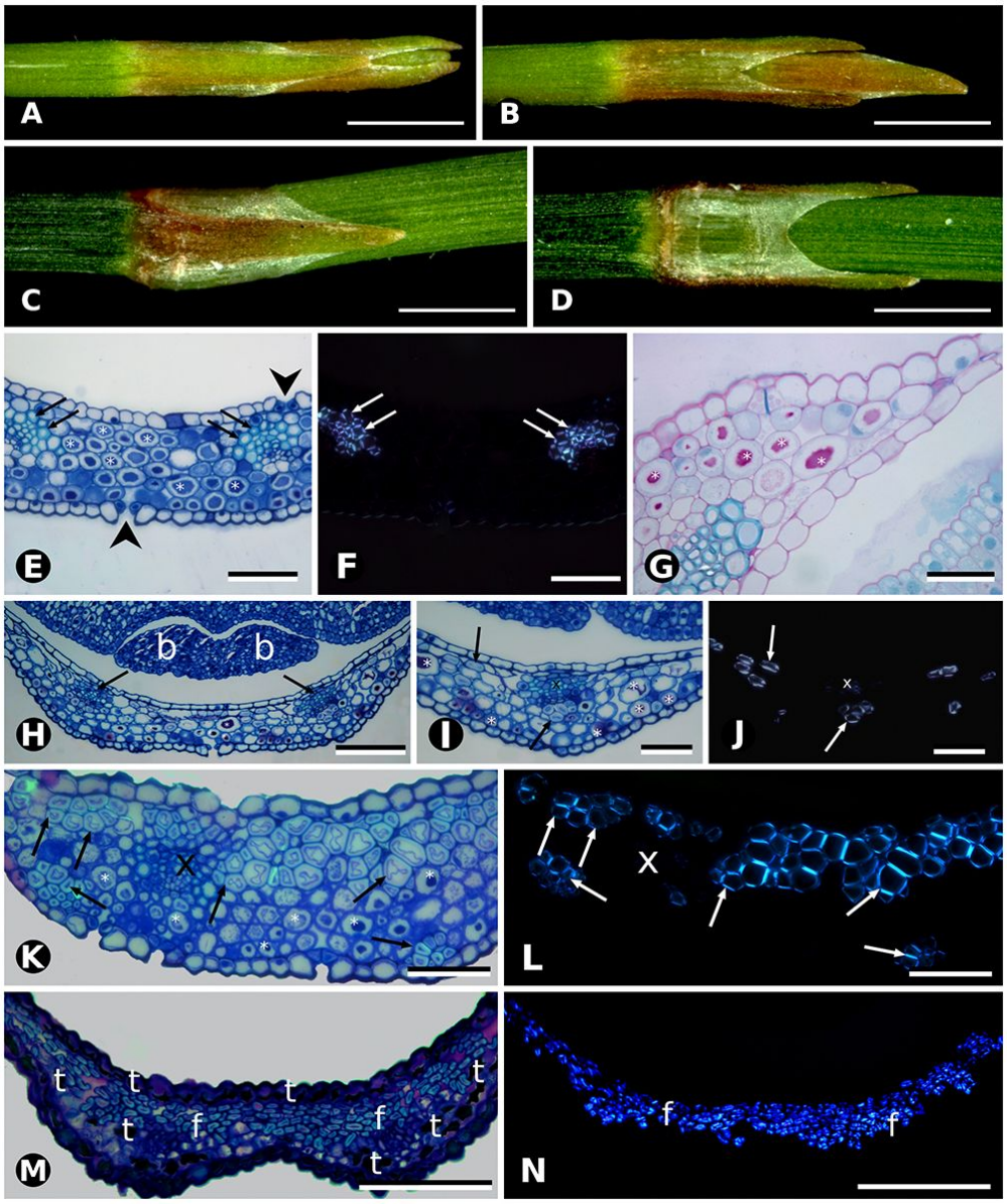

Figure 7

Comparative leaf morphology and anatomy of Ephedra in this study. (A-D) Overview of the morphology of E. tweediana leaves observed under a stereomicroscope. (A-B) Stem apex showing leaves from the first and second nodes in frontal and lateral views, respectively. (C-D) Detail of the fifth node from the stem apex showing developing leaves in frontal and lateral views, respectively. Note the development of the lateral, papiraceous zone. (E-G) E. tweediana (male individual). (E) Toluidine Blue O and PAS staining. Mucilage cells (*) are present throughout the mesophyll, cellulosic fibers (arrows) are associated with vascular bundles, and stomata are present on both leaf surfaces (arrowheads). (F) Polarized light microscopy of section in (E) showing the birefringence and distribution of cellulosic fibers (arrows). (G) positive PAS staining of mucilage in mesophyll cells. (H-J) E. tweediana (female individual). (H) General overview, arrows indicate vascular bundles, two axillary buds (b) are visible and mucilage cells (*) are distributed throughout the mesophyll. (I) High magnification of the vascular bundle in (D), showing cellulosic fibers (arrows) associated with the bundle and also distributed throughout the mesophyll. (J) Polarized light microscopy of section in (I) showing the birefringence of xylem cells (x) and cellulosic fibers (arrows). (K) E. triandra (male individual), with a different pattern from that found in E. tweediana: cellulosic fibers (arrows) are associated with vascular bundles, and also present in bundles abaxially and in layers adaxially. Mucilage cells are found in multiple layers on the abaxial surface. (L) Polarized light microscopy of section in (K) showing the distribution and birefringence of the cellulosic fibers. (M) E. multiflora (female individual) with tannin cells (t) in the adaxial epidermis and also distributed in one or two

layers on the abaxial face. Cellulosic fibers (arrows) differentiate in several adaxial layers in the mesophyll. (L) Polarized light microscopy of section in (K) showing the distribution and birefringence of the cellulosic fibers. Xylem (x), mucilage cells (*). Scale bars: 1 mm (A-D), 100 µm (E-F, K-N); 50 µm (G, I-J); 200 µm (H).

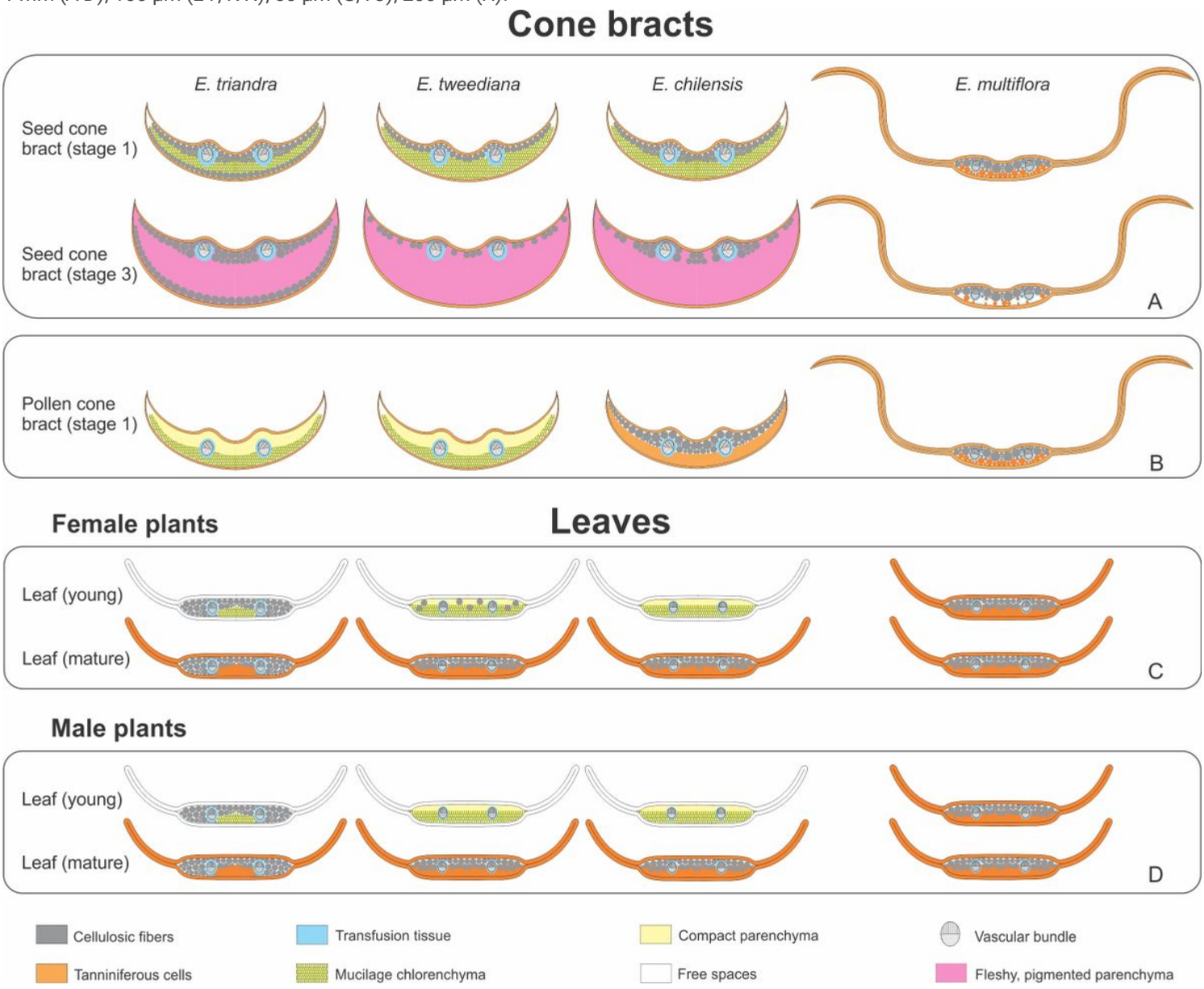

Figure 8

Summary diagrams of leaf and bract anatomy observations for Ephedra chilensis, E. multiflora, E. triandra, and E. tweediana. (A) Seed cone bracts at stage 1 (first line) and 3 (second line). (B) Pollen cone bracts at stage 1. (C) Leaves from female plants: at the second node (young, first line) and at the 5th-6th node (mature, second line). (D) Leaves from male plants: at the second node (young, first line) and at the 5th-6th node (mature, second line). Refer to figure inset for the meaning of colors and symbols.

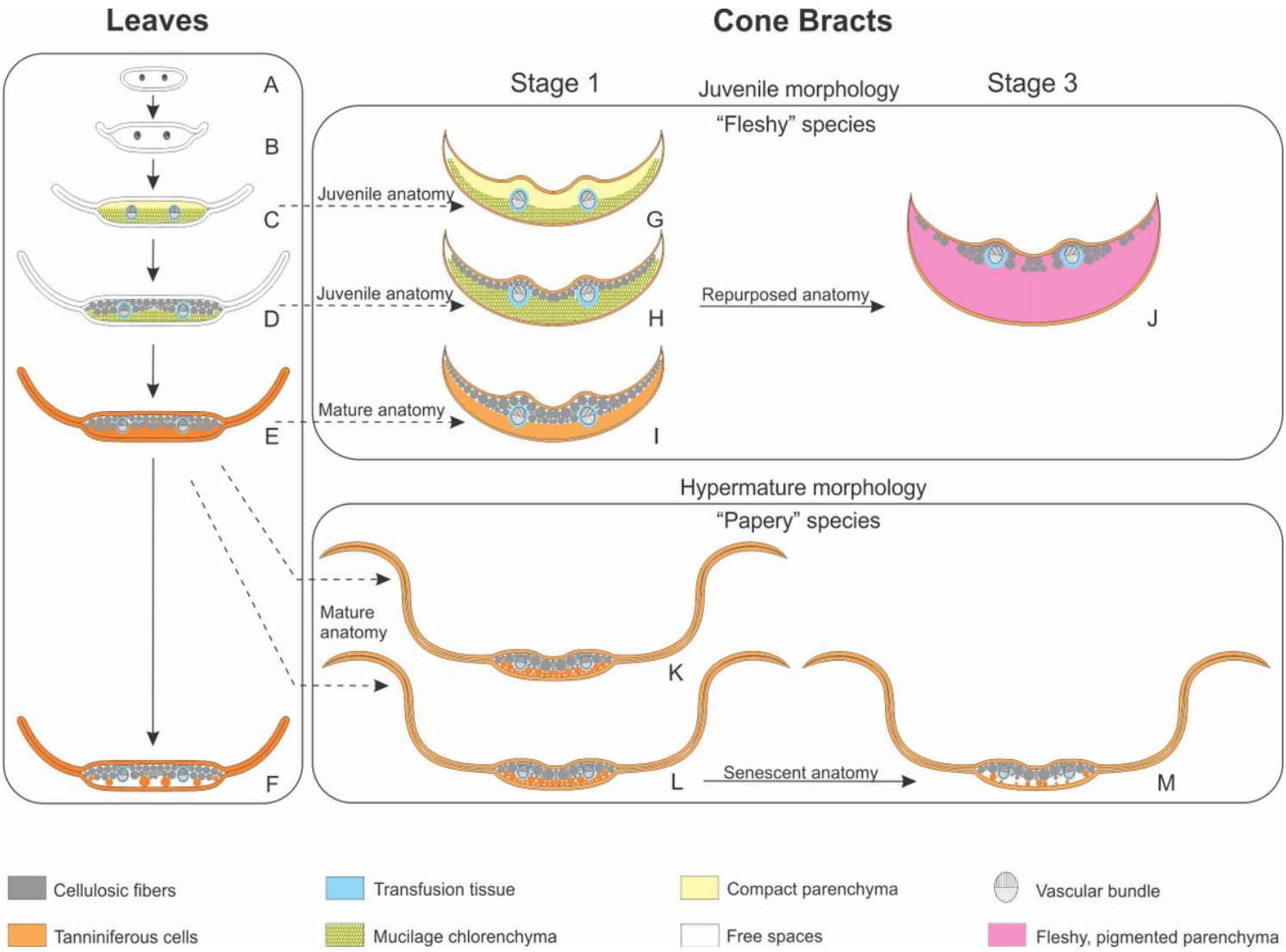

Figure 9

Cone bracts from leaves: Evolutionary developmental model for the repurposing of anatomical features from vegetative leaves to reproductive bracts in Ephedra (Gnetales). (A-F) Generalized leaf development across the four species studied. (G) Anatomy of pollen cone bracts of Ephedra triandra and E. tweediana (stage 1). (H) Generalized anatomy of fleshy seed cone bracts (stage 1). (I) Anatomy of pollen cone bracts of E. chilensis (stage 1). (J) Generalized anatomy of fleshy seed cone bract (stage 3). (K) Anatomy of pollen cone bract of E. multiflora stage 1). (L-M) Anatomy of seed cone bract of E. multiflora at stage 1 and 3 respectively. Solid line arrows connect stages of development. Broken line arrows indicate corresponding anatomies between stages of leaf development and bract structure. Bracts of fleshy species are grouped by their juvenile external morphology (reduced hyaline margins). Bracts of the papery species are grouped by their hypermature external morphology (widely developed hyaline margins). Refer to figure inset for the meaning of colors and symbols.

Supplementary Files

This is a list of supplementary files associated with this preprint. Click to download.

- Additionalfile1.jpg
- Additionalfile2.docx
- Additionalfile3.docx